Analyzing Relativistic Effects around Black Holes: XMM observations of Cygnus X-1

Image: ESA

Thomas Dauser[1], Refiz Duro[1], Jörn Wilms[1], K. Pottschmidt[2], M. A. Nowak[3], S. Fritz[1,4], E. Kendziorra[4], M. G. F. Kirsch[5], C. S. Reynolds[6], R. Staubert[4]

[1]ECAP, [2]CRESST/UMBC/NASA-GSFC, [3]MIT, [4]IAAT, [5]ESA-ESOC, [6]UMD

eMail: `thomas.dauser@sternwarte.uni-erlangen.de`

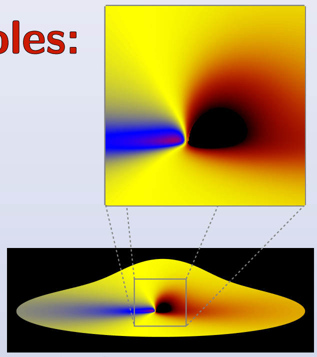

Image: Thomas Dauser

Abstract

We investigate the relativistic effects around black holes by spectral analysis of Modified Timing Mode observations of Cygnus X-1 with *XMM-Newton*. Simultaneous *RXTE* observations extend the energy to 120 keV and serve to constrain the continuum, which consists of a power law with exponential cutoff and a reflection component. As the majority of the reflected photons are emitted very close to the black hole, this component is relativistically smeared. Hence, the parameters of space time are imprinted in the spectrum, which is modeled by using the `relline` code. We find that Cygnus X-1 is fast spinning ($a \approx 0.9$), assuming the solution with a canonical emissivity of r^{-3} from a thin accretion disk. These results are explained in detail in a letter submitted to A&A (Duro et al., 2011). Using a new version of the `relline` code, we could also show that the data is equally well described if the emission is assumed to originate from the base of a jet at $7\,r_g$ above the black hole.

Simultaneous Observations of Cyg X-1

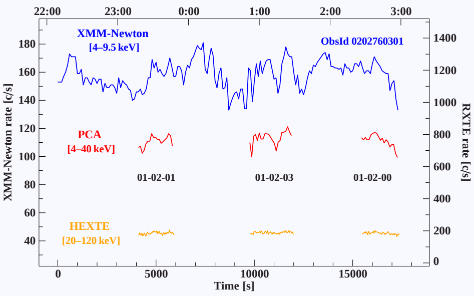

Figure 1 (Duro et al., 2011)**:** *XMM-Newton* and *RXTE* light curve of Cygnus X-1 on 2004 November 20/21. EPIC-pn data are shown in blue, PCA data in red, and HEXTE in orange.

For the analysis we use simultaneous *XMM-Newton* and *RXTE* observations performed 2004 November 20 and 21 (*XMM-Newton* ID 0202760301), while Cyg X-1 was in a transitional state between the hard state and the thermally dominated soft state (Fritz, 2008). Together, these instruments lead to a spectral covering of 4–120 keV. The EPIC-pn camera was operated in the Modified Timing Mode (see poster by Duro et al. and Duro et al. (2011) for more information), which yields the highest S/N observations of a galactic black hole around the iron Kα transition (4.6–9.5 keV). Hence, the broad energy coverage serves to fix the continuum efficiently and therefore allows for a better determination of the relativistically smeared reflection.

Jet Base vs. Corona Geometry

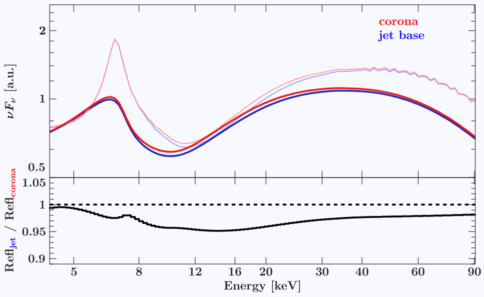

Figure 3: The reflection component assuming a canonical emissivity of r^{-3} (red) and the emission from the jet base, i.e. in the lamp post geometry, (blue). In both cases the light color indicates the intrinsic reflection, whereas the smeared reflection component is plotted full color.

Fitting showed that the data is equally well described if we assume that the photons irradiating the accretion disk originate from the base of a jet. Although some continuum parameters are slightly different, both models describe the data very well. As can be seen in the above figure, the shape of the smeared reflection does not change much and hence a slightly different power law index and norm can compensate for the changes. Therefore, we conclude that emission from a low jet base ($h = 7\,r_g$) can not be distinguished from the canonical model ($I \propto r^{-3}$) in the case of Cygnus X-1. This degeneracy is likely to be caused by the high ionization of the accretion disk, which results in a large Compton broadening of the intrinsic emission line.

The Full Model

	Jet Base	Corona ($\epsilon = 3$)	Corona
A_{pl}	$1.27^{+0.11}_{-0.12}$	$1.23^{+0.07}_{-0.08}$	$1.17^{+0.09}_{-0.08}$
Γ_{pl}	1.68 ± 0.02	1.670 ± 0.018	$1.663^{+0.019}_{-0.017}$
E_{fold} [keV]	330^{+123}_{-71}	287^{+74}_{-49}	289^{+80}_{-53}
A_{bb}	$(0.51 \pm 0.09) \times 10^4$	$(0.54 \pm 0.07) \times 10^4$	$(0.44^{+0.19}_{-0.07}) \times 10^4$
$A_{reflionx}$	$(1.6 \pm 0.4) \times 10^{-5}$	$(1.4 \pm 0.3) \times 10^{-5}$	$(1.2 \pm 0.3) \times 10^{-5}$
$Fe/Fe_\odot$	$1.6^{+0.7}_{-0.5}$	$1.7^{+0.5}_{-0.4}$	$1.6^{+0.5}_{-0.4}$
ξ [erg cm s^{-1}]	1279^{+424}_{-214}	1439^{+329}_{-202}	1740^{+334}_{-389}
$h[r_g]$	7 ± 2	–	–
a	$0.89^{+0.05}_{-0.11}$	$0.88^{+0.07}_{-0.11}$	-0.1 ± 0.4
ϵ	–	3	10^{+0}_{-6}
θ_O [deg]	34^{+4}_{-5}	32 ± 2	36^{+2}_{-4}
$F_{6.4\,keV}$[cgs]	$(0.68 \pm 0.19) \times 10^{-3}$	$(0.69^{+0.18}_{-0.20}) \times 10^{-3}$	$(0.6 \pm 0.2) \times 10^{-3}$
c_{HEXTE}	0.824 ± 0.007	$0.830^{+0.006}_{-0.005}$	0.830 ± 0.005
c_{EPIC}	0.790 ± 0.005	0.785 ± 0.004	0.785 ± 0.004
$s_{gainshift}$	1.024 ± 0.002	$1.0240^{+0.0019}_{-0.0018}$	$1.0230^{+0.0019}_{-0.0017}$
χ^2/dof	260/227	261/238	254/237
χ^2_{red}	1.15	1.10	1.08

Table 1: Parameters of the discussed best fit models. Uncertainties are at 90 % confidence.

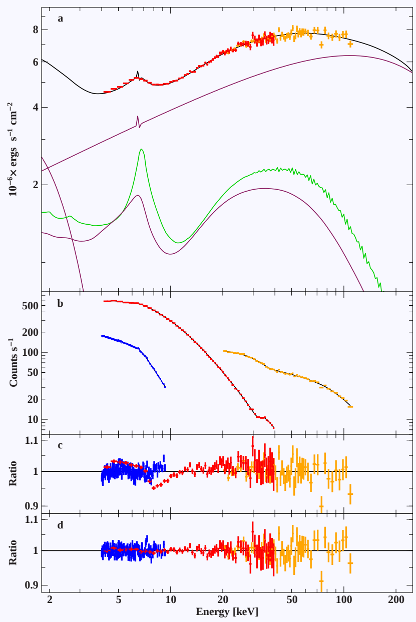

Figure 2 (Duro et al., 2011)**: a** Unfolded XMM-Newton and RXTE data and best fit model components. Green line: reflection continuum in the frame of the disk (note the strong Compton broadening; the "jitter" above 50 keV is due to the numerical resolution of the reflection model). Purple line: relativistically smeared reflection component. **b** Measured count rate spectra. **c** Residuals of the best fit setting the relativistic convolution to zero. **d** Best fit residuals including relativistic convolution.

The continuum model consists of an exponentially cutoff power law and takes the reflection self-consistently into account using the model `reflionx` (Ross & Fabian, 2005). In order to account for the relativistic smearing we convolve the reflected spectrum with the `relconv` model(Dauser et al., 2010). In addition, we include narrow Kα absorption lines from Fe XXV and Fe XXVI, as found in *Chandra*'s HETGS observation (ObsId 3814), which was at a similar flux level. Moreover a narrow emission line at 6.4 keV of neutral iron (as observed by Hanke et al., 2009) and a soft excess with $T = 0.5$ keV was added. Additionally a gain shift of the form $E_{real} = E_{obs}/s$ had to be applied for the EPIC-pn data, in order to be consistent with the narrow emission and absorption lines found in available *Chandra* measurements. See Duro et al. (2011) and the poster of Duro et al. "*X-ray Loading, Gainshift and (Modified) Timing Mode of XMM-Newton's EPIC-pn*" for more details.

We assume the reflected photons either to originate from a corona above a canonical, thin accretion disk ($I \propto r^{-3}$, Shakura & Sunyaev, 1973) or to be emitted from the base of a jet, i.e. in the lamp post geometry (e.g., Martocchia & Matt, 1996). The latter geometry is calculated by a new implementation of the `relline` model (Dauser et al., in prep.). Moreover a fit was performed, letting the disk emissivity parameter ϵ free ($I \propto r^{-\epsilon}$). All three models result in equally good fits to the data.

The Spin of Cygnus X-1

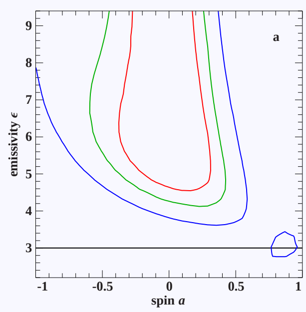

Figure 4 (Duro et al., 2011)**:** χ^2 significance contours for the corona geometry, based on $\Delta\chi^2 = 2.30$, 4.61, and 9.21. Two minima are apparent, one indicating a low spin black hole at an unphysically large ϵ, and one indicating an almost maximally spinning black hole consistent with emission from a thin accretion disk ($\epsilon = 3$).

Most best-fit parameters are consistent between all three fits. Letting the emissivity free in the coronal model yields unphysically high values at low spin of the black hole. Given that most physical scenarios for very steep emissivity profiles such as strongly torqued accretion disks (Agol & Krolik, 2000) also require high a, the high spin solution is preferred on physical grounds. This argument is strengthened by the fits in the lamp post geometry, which also lead to high a. Moreover, the solution of a rapidly spinning black hole is consistent with spin measurements from the accretion disk continuum (Gou et al., 2011).

Cygnus X-1 is therefore plausibly close to maximally rotating.

Acknowledgments & References

This work was partly supported by the European Commission under contract ITN215212 "Black Hole Universe" and by the Bundesministerium für Wirtschaft and Technologie under Deutsches Zentrum für Luft- und Raumfahrt grants 50 OR 0701 and 50 OR 1001. This paper is based on observations obtained with *XMM-Newton*, an ESA science mission with instruments and contributions directly funded by ESA member states and NASA. We thank M. Díaz-Trigo for useful discussions on the CTE effects, M. Hanke for the *Chandra* extractions, and J. E. Davis for developing the `slxfig` module used for plotting all figures.

Agol E., Krolik J.H., 2000, ApJ 528, 161
Dauser T., Wilms J., Reynolds C.S., Brenneman L.W., 2010, MNRAS 409, 1534
Duro R., Dauser T., Wilms J., et al., 2011, A&A submitted
Fritz S., 2008, Dissertation, IAAT
Gou L., McClintock J.E., Reid M.J., et al., 2011, ApJ submitted
Hanke M., Wilms J., Nowak M.A., et al., 2009, ApJ 690, 330
Martocchia A., Matt G., 1996, MNRAS 282, L53
Ross R.R., Fabian A.C., 2005, MNRAS 358, 211
Shakura N.I., Sunyaev R.A., 1973, A&A 24, 337

Friedrich-Alexander-Universität Erlangen-Nürnberg

ERLANGEN CENTRE FOR ASTROPARTICLE PHYSICS